THE ASTRONOMICAL JOURNAL, 115:1076–1082, 1998 March

COLLINDER 110: AN OLD OPEN CLUSTER IN MONOCEROS

D. W. DAWSON[1]
Department of Physics, Astronomy, and Meteorology, Western Connecticut State University, Danbury, CT 06810; dawson@wcsu.ctstateu.edu
AND
P. A. IANNA[1,2]
Department of Astronomy, University of Virginia, Box 3818, Charlottesville, VA 22903; pai@virginia.edu
Received 1997 August 11; accepted 1997 December 1

ABSTRACT

Results of photoelectric *UBVRI* photometry of 78 stars and photographic PDS and CCD photometry for 437 stars are presented for Collinder 110, an old open cluster at low Galactic latitude. Proper motions obtained from Lick Sky Survey plates were used to identify 39 stars as foreground objects. The cluster's reddening, distance, and age are estimated as $E(B-V) = 0.50 \pm 0.03$ mag, $r = 1950 \pm 300$ pc, and $t = 1.4 \pm 0.3$ Gyr, assuming a solar metal abundance.

Key words: open clusters and associations: individual (Collinder 110)

1. INTRODUCTION

Collinder 110 is a moderately rich open cluster (III1m; Trumpler 1930) located at equatorial coordinates $\alpha = 6^h38^m.4$, $\delta = +2°01'$ (J2000.0) and Galactic coordinates $l = 210°$ and $b = -2°$. It was listed by King (1964) as one of a group of open clusters suspected of great age but was omitted from the list of old clusters of Phelps, Janes, & Montgomery (1994).

The only photoelectric work on Cr 110 prior to this study was reported by Tsarevskii & Abakumov (1971), who obtained *UBV* photographic photometry for 120 stars out of 250 in a 5° field centered on Cr 110. Their main sequence extended to $V = 14$. Their cluster color-magnitude diagram (CMD) displayed a well-populated giant branch and a "clump" of stars near $V = 13.5$ and $B-V = 1.55$. They derived a color excess $E(B-V) = 0.55 \pm 0.05$ mag, a distance $r = 2.75 \pm 0.4$ kpc, and an age of about 3 Gyr.

As an open cluster of Gyr age, Collinder 110 is of interest to studies of stellar evolution and star formation. We decided to obtain photometry of more and fainter stars in the cluster field so as to refine the estimates of its observational parameters. Because of the low Galactic latitude of Cr 110, it was necessary to attempt some segregation of foreground stars on the basis of proper motions.

2. PHOTOELECTRIC OBSERVATIONS

Photoelectric photometry on the Johnson *UBV* and Cousins *RI* systems was obtained for 49 stars in the cluster field using the 0.9 and 1.5 m telescopes at Cerro Tololo Inter-American Observatory and the 1.3 m telescope at Kitt Peak National Observatory. *UBVRI* standard stars from Cousins (1974), Graham (1982), and Landolt (1983) were used in the photometric calibrations. The magnitudes and color indexes are listed in Table 1. Standard deviations of these calibrations were 0.011, 0.006, 0.016, 0.006, and 0.008 mag for V, $B-V$, $U-B$, $V-R$, and $R-I$, respectively.

Some CCD frames of a central portion of the cluster were also obtained, in the B and V filters, at the prime focus of the Anglo-Australian Telescope under the AAO service observing program. The CCD was a 512 × 320 pixel RCA chip calibrated using E-region standards (Graham 1982). The APEX photometry code of E. B. Newell at the Mount Stromlo Observatory was used to extract magnitudes. Therefore, also listed in Table 1 are V and B magnitudes and a $B-V$ color index (reported to 0.01 mag accuracy) for 29 stars in the CCD frames.

3. PHOTOGRAPHIC PHOTOMETRY

The plate materials used for photographic photometry are listed in Tables 2 and 3. *UBV* plates were obtained at CTIO on the 1.0 m Yale Telescope at the f/7.5 Ritchey-Chrétien focus. Additional plates were obtained with the 1.0 m f/13.5 astrometric reflector at the Fan Mountain Observatory of the University of Virginia.

Figure 1 is a chart of the Cr 110 field covering approximately 10′. Throughout, we refer to stars according to quadrant-and-ring notation; e.g., star 1282 is number 82 in ring 2 of quadrant I. Initially, two regions were used: a central circle of 250″ radius surrounded by a ring of 250″ thickness. However, when we performed the proper-motion study, another ring of 136″ thickness was added because of the crowding of star images in the inner regions as seen on the smaller scale Sky Survey plates. Some stars in the outer ring have proper motions but not photometry, and vice versa for some stars in the inner regions.

The CTIO and Virginia plates were measured at the PDS microdensitometer facility at Yale University. A window 20″ on a side (40″ for the Virginia plates) was raster-scanned across each image with a 15 μm scan step (30 μm for the Virginia plates) and 25% scan overlap, producing a 40 × 40 sample array for each star. Following the procedure outlined by Lee & van Altena (1983), we fitted the results of each scan to a binormal distribution of the form

$$D(x, y) = D_0 \exp\left[-(x^2 + y^2)/S_x S_y\right] + B ,$$

where B is the base density level. In most cases $S_x = S_y$, indicating round images; poor seeing is apparent as an increase in both values, and $S_x \neq S_y$ indicates trailing. The

[1] Visiting Astronomer, Cerro Tololo Inter-American Observatory and Kitt Peak National Observatory, National Optical Astronomy Observatories, operated by the Association of Universities for Research in Astronomy, Inc., under cooperative agreement with the National Science Foundation.
[2] Visitor, Mount Stromlo and Siding Spring Observatories, Canberra, Australia.

TABLE 1

PHOTOELECTRIC PHOTOMETRY

Star	x	y	V	B	U	$U-B$	$B-V$	$V-R$	$R-I$	$V-I$	n
1103.....	20.0507	−1.2985	14.998	16.285	...		1.287	0.831	0.775	1.607	1
1138.....	11.6021	1.1009	12.468	13.819	14.834	1.015	1.351	0.726	0.708	1.434	1
1148.....	10.4161	3.9953	12.965	14.508	15.670	1.162	1.543	0.845	0.772	1.618	1
1152.....	13.9354	6.0338	11.868	13.224	14.415	1.191	1.356	0.715	0.658	1.373	1
2117.....	12.0401	14.6301	15.245	15.992	...		0.747	0.455	0.453	0.908	1
2118.....	13.3480	13.3371	15.40	17.16	...		1.76				1, 2
2120.....	14.4648	13.1031	...	17.41	...						2
2121.....	14.7787	13.4435	...	17.45	...						2
2122.....	14.4475	14.8561	...	16.72	...						2
2123.....	14.9968	15.2253	15.78	16.52	...		0.74				1, 2
2124.....	17.8785	12.7196	16.249	17.037	...		0.788	0.481	0.466	0.947	2
2127.....	18.4415	13.0830	...	17.47	...						2
2128.....	17.4580	16.9112	14.65	15.36	...		0.71				1, 1
2129.....	19.0379	13.7071	13.625	14.993	15.983	0.990	1.368	0.721	0.765	1.489	1
2130.....	19.2773	13.0515	15.31	16.13	...		0.82				1, 2
2131.....	19.7280	11.4131	...	15.15	...						1
2133.....	19.8936	14.3672	...	17.00	...						2
2134.....	19.7844	17.7826	14.64	15.51	...		0.87				1, 2
2136.....	20.3761	12.8973	...	16.71	...						2
2137.....	20.2443	15.1683	...	16.32	...						2
3102.....	21.4433	18.6468	13.72	14.49	...		0.77				1, 1
3103.....	21.3622	15.8886	...	15.87	...						2
3104.....	21.5549	17.8069	...	16.09	...						2
3105.....	21.6422	15.5111	...	17.36	...						2
3106.....	21.9892	15.9668	...	16.19	...						2
3107.....	22.5456	17.7781	11.465	12.681	13.858	1.177	1.216	0.751	0.629	1.382	1
3108.....	21.7265	12.2506	...	15.45	...						2
3109.....	21.7606	11.9452	...	16.79	...						2
3110.....	21.9032	13.1571	16.718	17.538	...		0.820	0.536	0.520	1.056	2
3111.....	23.3142	18.1479	15.15	15.75	...		0.60				1, 2
3112.....	23.1750	15.4139	14.889	15.632	...		0.743	0.489	0.558	1.046	1
3113.....	22.7171	13.8240	...	17.04	...						2
3115.....	22.8106	12.4995	...	16.61	...						2
3118.....	23.6589	12.4372	14.94	15.80	...		0.86				1, 2
3119.....	24.6235	14.4400	...	16.11	...						2
3120[a].....	24.2736	13.1778	...	15.87	...						2
3122.....	24.0902	11.7673	...	14.79	...						1
3123.....	26.2165	16.4611	13.233	14.789	16.415	1.626	1.556	0.841	0.764	1.601	1
3130.....	22.1585	7.7938	13.037	14.418	15.547	1.018	1.381	0.772	0.722	1.494	2
3144.....	27.5464	7.4063	13.505	14.865	16.000	1.135	1.360	0.748	0.717	1.460	1
4111.....	24.2912	1.7280	12.111	13.949	15.988	1.999	1.838	1.004	0.940	1.949	2
4132[a].....	21.4607	0.6524	13.877	15.327	16.438	1.111	1.450	0.832	0.766	1.598	1
4134.....	21.1251	−1.8348	15.095	15.701	...		0.606	0.355	0.389	0.742	1
1201[b].....	20.2618	−15.9254	11.283	11.978	12.069	0.091	0.695	0.401	0.399	0.801	1
1212.....	17.5508	−10.6961	13.115	14.671	16.137	1.466	1.556	0.889	0.845	1.735	2
1218.....	15.9151	−10.1518	11.470	13.654	16.008	2.354	2.184	1.283	1.261	2.543	1
1238.....	14.9	−6.5	13.872	15.208	16.142	0.934	1.336	0.776	0.744	1.519	1
1244.....	8.1709	−14.7947	13.294	14.127	14.539	0.412	0.833	0.450	0.479	0.928	1
1278.....	−3.8192	−1.4083	13.507	14.789	15.710	0.921	1.282	0.748	0.731	1.477	2
2202.....	6.1507	6.1119	11.800	13.685	15.843	2.158	1.885	1.049	0.986	2.035	4
2218.....	2.5106	13.1147	12.984	14.368	15.418	1.050	1.384	0.777	0.754	1.532	2
2223.....	1.4114	17.9106	13.462	14.809	15.844	1.035	1.347	0.719	0.736	1.455	2
2237.....	12.9822	16.4249	15.135	15.897	...		0.762	0.476	0.496	0.971	2
2240.....	13.0051	17.5789	14.29	15.00	...		0.71				1, 1
2241[a].....	12.6773	18.1782	...	16.17	...						2
2242.....	12.4433	19.2223	14.943	15.674	...		0.731	0.407	0.462	0.868	1
2243.....	12.0304	19.9312	15.411	17.239	...		1.828	1.036	1.046	2.083	1
2256.....	15.5596	23.9985	13.334	14.733	15.931	1.198	1.399	0.839	0.757	1.597	1
3239.....	41.8850	11.3693	16.019	18.096	...		2.077	1.233	1.167	2.401	2
3243.....	41.5829	9.8688	15.396	16.171	...		0.775	0.482	0.514	0.994	2
3244.....	38.8809	9.3045	13.752	15.140	16.223	1.083	1.388	0.769	0.738	1.507	4
3249.....	35.5964	7.3948	13.664	15.033	16.131	1.098	1.369	0.775	0.731	1.506	2
4204.....	35.0952	4.9494	12.703	14.198	15.626	1.428	1.495	0.826	0.764	1.590	3
1306.....	13.7916	−21.9108	12.625	14.895:	17.408:	2.513:	2.270:	1.261	1.204	2.465	2
1310.....	−1.6444	−17.2081	13.766	16.320	18.716	2.396	2.554	1.354	1.237	2.588	2
1311.....	1.9135	−12.4425	13.888	15.392	16.444	1.052	1.504	0.799	0.760	1.558	1
1319[a].....	−9.1428	4.5829	12.895	14.425	15.745	1.320	1.530	0.820	0.804	1.624	3
1382.....	2.9	−25.4	13.633	15.016	16.050	1.034	1.383	0.755	0.765	1.520	2
S-3	−7.1243	8.0367	13.545	15.954	18.096	2.142	2.409	1.436	1.349	2.787	1
S-4	−6.4223	8.1056	11.890	13.795	15.759	1.964	1.905	1.038	0.934	1.973	1
S-5	−4.7771	22.8642	12.400	13.770	14.984	1.214	1.370	0.703	0.640	1.344	1
S-6	4.1148	28.3516	12.698	13.767	14.632	0.865	1.069	0.561	0.504	1.067	1
S-7	4.3585	36.0644	12.956	14.500	15.867	1.366	1.544	0.840	0.861	1.701	2

TABLE 1—*Continued*

Star	x	y	V	B	U	$U-B$	$B-V$	$V-R$	$R-I$	$V-I$	n
S-8	13.0537	39.1141	13.366	15.046	16.353:	1.307:	1.680	0.894	0.819	1.715	1
S-9	15.2189	41.1142	13.471	15.115	16.413:	1.298:	1.644	0.903	0.839	1.744	1
S-10	1.0497	42.2364	13.306	14.765	15.867	1.102	1.459	0.803	0.752	1.555	1
"A"	−4.4	39.3	7.704	8.954	10.102	1.148	1.250	0.673	0.616	1.289	3
"B"	−5.3	42.1	9.150	10.182	11.015	0.833	1.032	0.535	0.505	1.040	3

[a] Has faint, close companion.
[b] Close double.
NOTE.—Star 1311 = S-11; star 1319 = S-2; star "A" = SAO 114212 = BD +2°1332 (K0; m_v = 8.3).

TABLE 2

PLATE MATERIALS: CLUSTER PHOTOGRAPHS

Plate	Observatory	Plate/Filter	Date (1983)	Exposure (minutes)	H.A. (end)	Clear D	Remarks
3654.....	CTIO	103a-D + GG495	Jan 15	60	W0:02	0.42	Slightly elongated images
3664.....	CTIO	103a-D + GG495	Jan 17	60	E1:14	0.40	Slightly elongated images
3656.....	CTIO	IIa-O + GG385	Jan 15	30	W2:33	0.39	
3661.....	CTIO	IIa-O + GG385	Jan 16	50	W0:23	...	Slightly elongated images
Va265.....	UVa	IIa-O + GG395	Jan 19	120	W1:00	0.35	Poor seeing
Va318.....	UVa	IIa-O + GG395	Mar 2	180	W0:26	0.30	
3655.....	CTIO	IIa-O + UG2	Jan 15	60	W1:28	0.24	Slightly underexposed
3662.....	CTIO	IIa-O + UG2	Jan 16	90	W2:15	0.18	Soft images
3666.....	CTIO	IIa-O + UG2	Jan 17	70	W1:25	...	

Virginia plates have a larger scale than the CTIO plates, and their images are somewhat larger. Positional repeatability was ±5 μm. An instrumental magnitude for each image was generated from the volume of the distribution out to 2 σ. Star images for which the density distribution had a flat top (i.e., saturated) were flagged in the output data. Some bright stars on the photographs (probable cluster nonmembers) were also scanned to evaluate the effects of saturation on the derived magnitudes; images of most stars in the cluster field, including the photoelectric standards, were free of significant saturation effects.

Because of the crowding of faint stars in the inner region, not all the program stars are labeled in Figure 1. Therefore, the (x, y)-coordinates in millimeters for all stars studied are listed in Table 1 and in Table 5 below. The coordinate system was based on scanning of CTIO V plate 3664; in this system, the cluster center is at (x, y) ~ (20.8, 6.4) and the most positive (+, +) coordinates lie in quadrant III. Stars in ring 3 were not scanned on plate 3664 but were scanned on the Lick plates, so linear transformations in x and y were used with coordinates on Lick V plate 5848 to derive equivalent coordinates on the CTIO plate for stars able to be scanned on both; the transformed (x, y)-coordinate standard deviations are ±28.3 and ±22.5 μm. Finally, approximate coordinates were estimated by eye from CTIO plate 3664 for a few stars misidentified or not scanned on the Lick plates; these are listed only to 0.1 mm.

TABLE 3

PLATE MATERIALS: LICK PROPER MOTION (SKY SURVEY) PLATES

Plate	Emulsion	Date
AB1839.....	103a-O	1951.08
AB2138.....	103a-O	1952.07
AB5848.....	103a-O	1958.16
AB5857.....	103a-O	1958.16
AB8395.....	103a-O	1977.04
AB9689.....	103a-O	1984.97
AY5848.....	103a-G	1958.16
AY8397.....	103a-G	1977.04
AY9689.....	103a-G	1984.98

NOTE.—B plate scale = 55.″14 mm^{-1}; V plate scale = 55.″07 mm^{-1}.

For each ring and quadrant, an estimate of image blending or contamination was made by comparing the base density value for that star with the average base density for that section of the plate. Images with values 2 σ or more higher than the average were rejected, and their magnitudes were not used in any further analysis. The numbers of stars sampled on each plate, and the fraction rejected, are listed in Table 4. The fraction tends to be lower for the U plates because stars' images were generally not as deeply exposed.

Repeatability of the PDS magnitudes was tested by scanning a dozen photoelectric standards on each plate on several occasions during the measurement of the program stars. The brightest stars showed repeatability to about 0.002 mag as long as the images had no obvious saturation; for the faintest standards (B ~ 17), ±0.004 mag was a more typical scatter.

The microdensitometer magnitudes were calibrated against photoelectric magnitudes for each plate, with CCD magnitudes (Table 1) used as secondary calibrators. Usually, a cubic polynomial represented the overall calibration with reasonable accuracy. Color corrections were also determined, by analyzing deviations from the overall fit as functions of $B-V$; the CTIO plates showed smaller corrections than the Virginia plates. The U color dependence proved difficult to evaluate, being near the level of observational scatter; therefore, we decided to err on the conservative side and report the $U-B$ color indexes uncorrected for any color dependence, recognizing however that there probably is a small one (at the few hundredths magnitude level, lower for the bluest stars and higher for the reddest, as best we could evaluate the trend). Mean magnitudes in V, B,

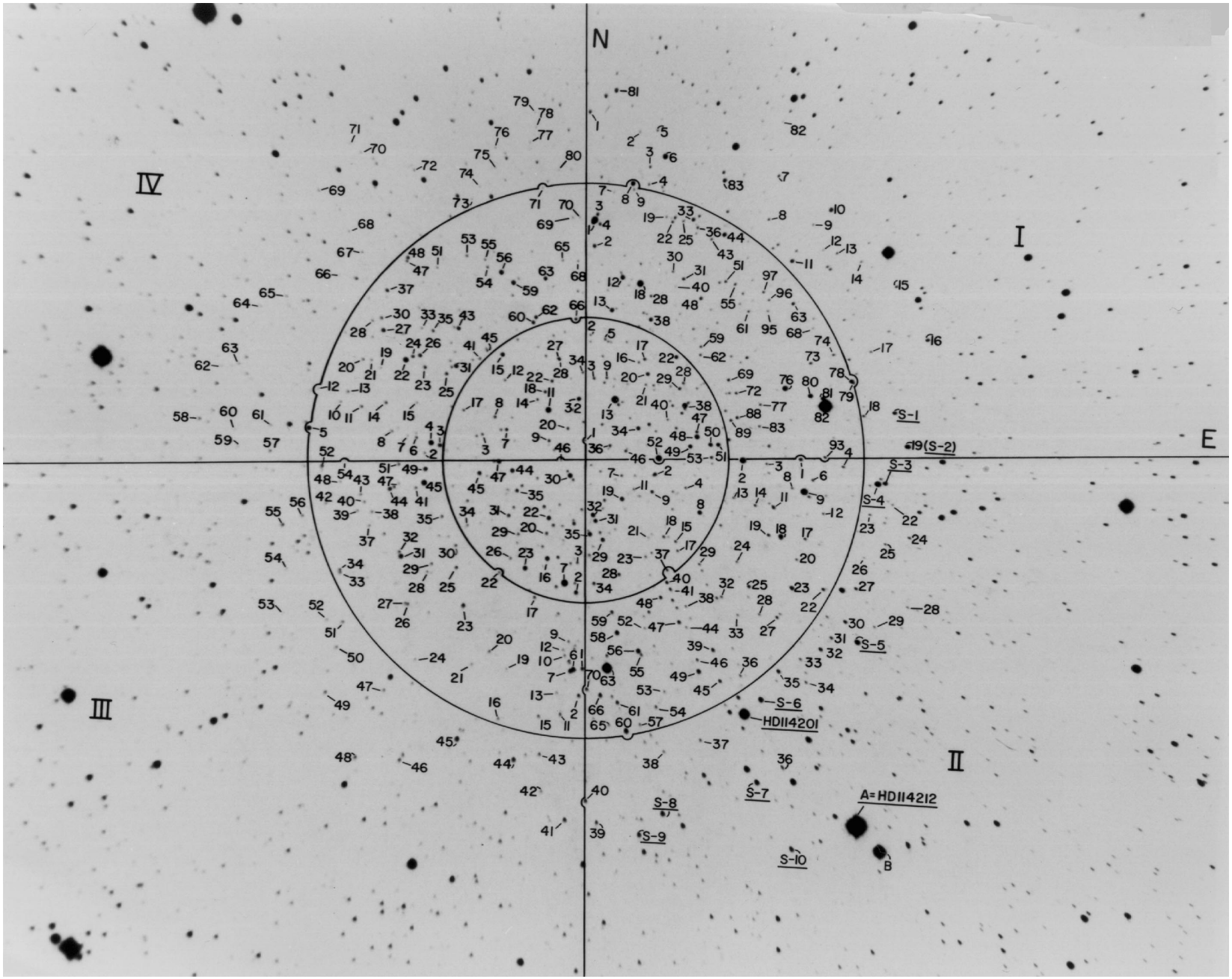

FIG. 1.—*V* identification chart for Collinder 110. North is up, and east is to the right. The central circle has a radius of 250″, while the second ring has the same thickness. The boundary of ring 3 is not delineated but is about 136″ beyond that of ring 2.

TABLE 4

STARS REJECTED FOR HIGH BACKGROUND VALUES

Plate	Usable Stars	Rejected (%)
3654 (*V*)	400	37 (8.5)
3664 (*V*)	401	36 (8.2)
3661 (*B*).....	401	36 (8.2)
Va265 (*B*).....	400	37 (8.5)
Va318 (*B*).....	396	41 (9.4)
3655 (*U*)	417	20 (4.6)
3662 (*U*)	416	21 (4.8)
3666 (*U*)	407	29 (6.7)

and *U* were obtained by combining results from the individual plates in a sum weighted by the reciprocals of the fit variances. Typical scatters (σ) were ± 0.08, ± 0.07, and ± 0.085 mag for single *V*, *B*, and *U* plates, respectively, without color corrections and ± 0.044 and ± 0.046 mag (in *V* and *B*) with color corrections.

Results of photographic photometry are listed in Table 5. Magnitudes or color indexes for which the internal variation of the estimates exceeds 0.10 mag are followed by a colon.

4. PROPER MOTIONS

Since Cr 110 is more than 1 kpc distant, stars with large proper motions are likely to be foreground stars instead of cluster members. Stars behind the cluster cannot readily be distinguished from members by proper motions. Nonetheless, identifying foreground stars is useful in cleaning up the CMD and estimating the amount of field star contamination.

Six *B* and three *V* plates of the Lick Sky Survey (Tables 2,

TABLE 5

PHOTOGRAPHIC DATA

Star	*x*	*y*	*V*	*B*−*V*	*U*−*B*	μ_x	μ_y	Remarks
1101	20.8058	4.4909	15.42	0.81	0.24	−0.10	0.52	
1102	20.4324	−5.3243	15.47	0.83	0.35:	−1.26	0.36	Foreground star
1103[a].....						−0.09	−0.96	
1104	19.2747	−3.3717	15.73	0.74	0.23	−0.03	0.81	
1105	19.0791	−4.9399	15.32	1.04	0.53			
1107	18.5227	−4.6685	16.07	0.84	0.16			
1108	19.0862	−0.9028	15.51	0.91	0.19			
1109	18.8834	−1.3581	15.10	0.75	0.28			
1110	17.0619	−4.7164	15.85	0.81	0.22	0.47	0.23	
1111	18.1544	−1.2594	16.13	0.82	0.05			
1112	18.2201	−0.5686	16.31	0.87	0.10			
1113	18.1059	0.6601	11.04					
1114	19.2487	2.9894	15.19	0.52	0.43	−0.32	0.65	
1115	16.8037	−1.3042	16.35	0.81	0.03	1.14	0.76	
1116	15.9064	−2.8626	15.44	0.75	0.30			
1117	15.3855	−3.1513	...			1.17	1.24	Foreground star
1119	17.4037	0.8704	16.08	0.77	0.13			
1120	15.0737	−17717	14.03	1.59	1.43	0.38	−0.67	
1121	15.2298	−0.7871	15.54	0.78	0.27	−0.74	−0.03	
1122	12.4581	−3.3900	13.78	1.39	1.02	0.38	0.22	
1123	14.5124	−0.7270	15.43	0.78	0.23			
1124	14.4503	−0.3318	16.40	0.82	0.09			
1125	14.0460	−0.8448	16.61	0.87	−0.06	−0.36	0.15	
1126	16.6438	2.3454	15.84	0.70	0.25	−0.22	−0.78	
1127	12.9219	−0.6691	15.79	1.10	0.64	0.63	0.74	
1128	11.7447	−0.9940	15.11	1.08	0.51	0.77	1.54	Foreground star
1129	12.0831	−0.4617	14.60	1.00	0.41	−0.34	−1.13	
1130	12.9492	0.6863	15.87	0.75	0.20			
1131	10.4642	−0.5175	15.76	0.79	0.25	−1.08	−0.15	
1132	12.7115	1.1239	15.30	0.77	0.33			
1134	15.8790	3.2938	13.71	1.39	1.04	−0.16	−0.09	
1135	14.8706	2.8997	14.57	1.38	0.97	−0.29	0.45	
1136	18.4829	4.9486	14.86	1.69	0.95			
1137	18.6339	5.2317	16.40					
1139	11.2559	0.8330	15.38	0.71	0.38			
1140	13.1479	2.4233	15.64	0.75	0.23	−0.82	0.50	
1141	11.5767	1.4154	15.73	0.76	0.22			
1142	11.8409	1.8111	14.82	0.97	0.23			
1143	14.2279	3.5371	15.83	0.76	0.23	0.28	0.00	
1144	10.4154	1.9630	15.81	0.87	0.53			
1145	12.3498	3.2179	15.19	0.78	0.31	−0.82	0.03	
1146	17.0066	5.4239	...			0.06	−0.14	
1147	10.4237	3.5229	14.77	0.63	0.43			
1149	11.0181	4.8907	13.64	1.41	1.06	0.01	−0.30	
1150	9.1393	4.6954	13.58	1.42	1.06			
1151	8.4281	4.6955	13.69	1.34	1.03			
1153	9.0277	5.8866	14.75	0.78	0.30	−0.24	−0.06	
2101	8.9406	6.4494	16.11	0.77	0.15			
2102	14.2627	7.5436	...					Blended with 2103
2103	14.2592	7.5419	13.92	1.43				Blended with 2102

NOTE.—Table 5 is presented in its entirety in the electronic edition of the Astronomical Journal. A portion is shown here for guidance regarding its form and content.

[a] See Table 1 for positions, *V* magnitude, and colors.

3) were analyzed at the Automated Measuring Engine (AME) facility at the University of California, Santa Cruz, by D. W. D. and T. Nakajima (Nakajima 1986). After initial position measurements with a Gaertner engine, each plate was placed onto the AME and the chosen images were scanned to determine their photometric centers. Images were chosen for AME measurement if their sizes were 50–250 μm and if no other images were found within 25 μm of their edges; this yielded 371 measurable stars. A search was conducted with a 60 μm scanning aperture over a (maximum) 400 μm square area of plate for each stellar image. The positional accuracy of the scans was ± 5 μm, which corresponds to $\pm 0''.28$ at the scale ($\sim 55''$ mm^{-1}) of the Sky Survey plates.

Magnitudes were also produced as a by-product of the AME scans, but were somewhat less accurate (~ 0.08 mag for V and ~ 0.11 mag for B) than those derived from PDS scans because of the larger plate scale and greater image crowding of the Sky Survey plates. As with the CTIO and Virginia plates, estimating the magnitudes involved determinations of color dependence and cubic polynomial fitting. V magnitudes and $B-V$ color indexes for the stars in ring 3 are listed in Table 5. We determined that 20% of the program stars in ring 1 and 23% of those in ring 2 could not be accurately measured because of blending.

In the last three columns of Table 5 are listed the x- and y-components (corresponding essentially to μ_α and μ_δ) of relative proper motion for the program stars, derived from six plate pairs (longest time interval: 33.89 yr) and expressed in units of arcseconds per century. These are displayed in the (μ_x, μ_y)-diagram of Figure 2. Most of the stars studied have motions that lie within a circle of radius $0''.6$ per century, and this is considered to be the level of the errors of the proper motions. Stars with proper motion in either coordinate of $\geq 1''.2$ per century were considered foreground stars.

Four stars in particular had large enough proper motions to be detected visually, while blinking plates taken in 1952 and 1977. These were stars 4224, 1381, 1382, and 3107. Crowding by nearby stars hindered accurate position measurements by AME. However, their proper motions (μ_x, μ_y) were visually estimated as ($-15''.7$, $2''.7$), ($0''.2$, $-4''.8$), ($-0''.9$, $-2''.0$), and ($4''.8$, $-5''.5$) per century, respectively, with uncertainties in μ_x and μ_y of $\pm 1''.8$ and $\pm 1''.6$ per century.

5. ANALYSIS OF THE DATA

The reddening of Cr 110 was obtained from the UBV two-color diagram using 22 stars with low proper motion (i.e., likely cluster members) and photoelectric photometry that fell on the giant branch. Following the discussion by Fernie (1963), we used a slope $X = 1$ for the reddening line. We derive $E(B-V) = E(U-B) = 0.53 \pm 0.04$ mag for the most reasonable fit range to the giant branch. The red star 1218 (which is very distant from the trends shown by the other stars) may have abnormal colors or may be variable.

The cluster CMD is shown in Figure 3. Only stars with μ_x or $\mu_y < 1''.2$ per century, those without available proper motions, and those without significant plate blending were used in constructing this figure. The clump of horizontal-branch stars is obvious at ($V \sim 13.6$, $B-V \sim 1.35$). There is a pronounced gap just above the main-sequence turnoff, which occurs at ($V \sim 15.4$, $B-V \sim 0.8$). The CMD of Cr 110 is very similar to that of NGC 7789 ($t \sim 2$ Gyr; Cannon 1970; Friel & Janes 1993; Jahn, Kaluzny, & Ruciński 1995). Cr 110 seems to have a fair number of blue stragglers. Alternatively, we might be observing another, younger stellar grouping along the same line of sight.

Castellani, Chieffi, & Straniero (1992) computed isochrones for open clusters of solar abundance, from the zero-age main sequence to the asymptotic giant branch. They found that the lower envelope of the clump had $M_V = 0.85 \pm 0.1$ mag for clusters with ages greater than 500 Myr. Simultaneously fitting the shape of the main-sequence turnoff and the magnitude level of the lower envelope of the

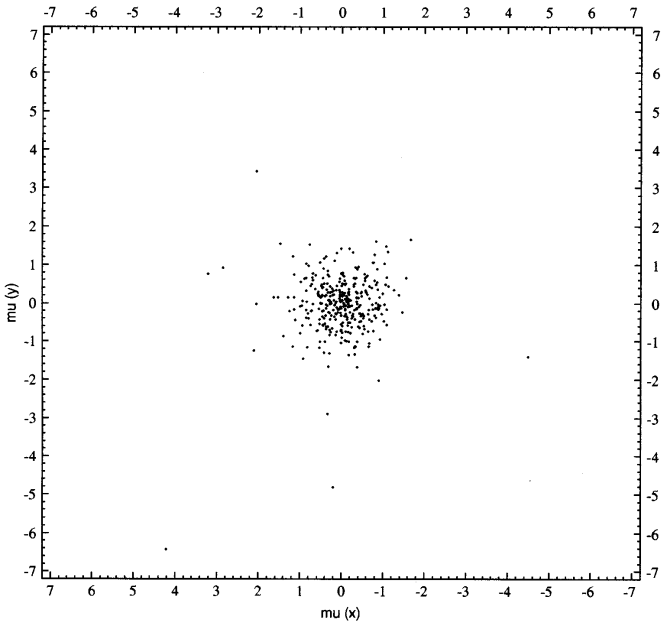

FIG. 2.—Proper-motion (μ_x, μ_y) diagram (arcsec per century) for stars in Cr 110 with measured proper motions. Only star 4224, with $\mu_x \sim 15''.7$ per century, is not plotted.

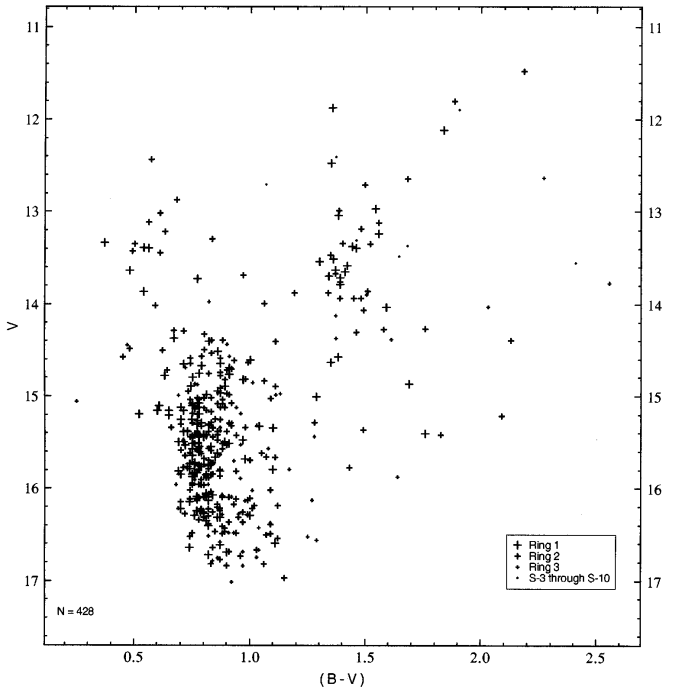

FIG. 3.—Color-magnitude diagram for Cr 110. Stars with high proper motion or saturated or blended images have been excluded.

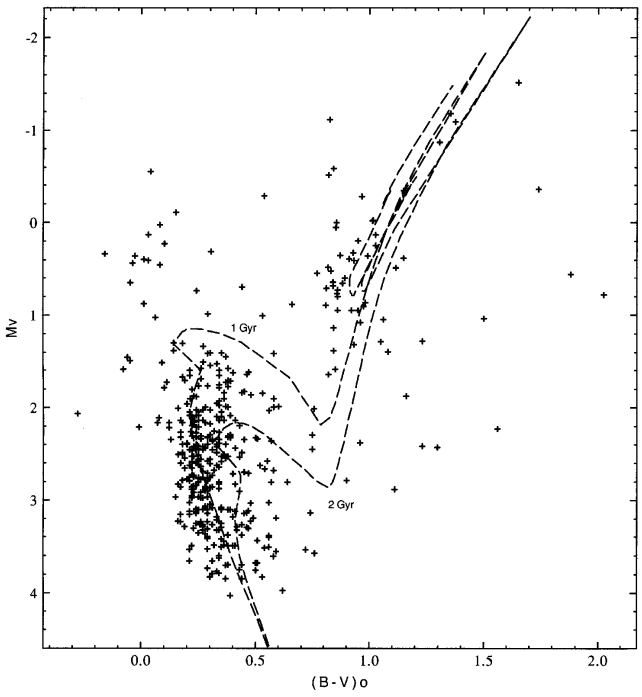

FIG. 4.—Observational H-R diagram for Cr 110. Corrections $E(B-V) = 0.53$ mag and $A_V = 1.59$ mag have been applied for interstellar extinction and obscuration and a distance modulus $V_0 - M_V = 11.4$ assumed. Superposed on the data are 1 and 2 Gyr isochrones from the models of Castellani, Chieffi, & Straniero (1992).

clump (but not its color; see below) to the isochrones allowed us to derive a reddening of 0.50 mag, $V_0 - M_V = 11.45$ mag, and a distance $r = 1950$ pc, with estimated uncertainties of ± 0.03 mag, ± 0.33 mag, and $^{+320}_{-270}$ pc, respectively. Figure 4 shows the observational H-R diagram of Cr 110 with 1 and 2 Gyr isochrones superposed.

Twarog, Anthony-Twarog, & Hawarden (1995) provided a comparison of canonical isochrone models and models incorporating convective core overshoot for a sample of old clusters, including NGC 2420 and Melotte 66. Their Figures 5 and 6 suggest that including core overshoot leads to isochrones that better match a cluster's main-sequence turnoff and subgiant branch. Twarog et al. also noted that the isochrones of Castellani et al. (1992) provided an adequate fit to the CMD of NGC 2420 only because they had not been normalized to the Sun's absolute magnitude and intrinsic color at $t = 4.6$ Gyr and had not been adjusted to the lower metallicity of that cluster. However, both the overshoot and nonovershoot models predict giant branches ~ 0.07–0.14 mag too red relative to observations; this is easily seen in our Figure 4 in the position of the clump versus the plotted isochrones.

Because the metallicity of Cr 110 is not yet known, and because of the noisy cluster CMD, we do not attempt a detailed comparison of the available isochrones here. However, the rounder turnoff regions of the core-overshoot isochrones would yield a somewhat better fit to the available data.

Our best estimate of the cluster's age is $t = 1.4 \pm 0.3$ Gyr. Aside from uncertainties in CMD fitting and theoretical considerations in the computation of isochrones, uncertainty in the age will also arise from our lack of knowledge of the helium abundance and metallicity, which will be determined only from a detailed spectral analysis of member stars. Nonetheless, Collinder 110 is comparable in age to other old open clusters. Phelps et al. (1994) used the CMD morphological age parameters δV (the magnitude difference between the main-sequence turnoff and the clump) and $\delta 1$ (the difference in color index between the bluest point at the luminosity of the main-sequence turnoff and that of the giant branch at a luminosity 1 mag brighter); we estimate from the CMD that $\delta V \sim 1.2$ and $\delta 1 \sim 0.64$, values similar to those for NGC 7789.

Many people provided material assistance, advice, and constructive criticism during this research. The authors wish to thank William van Altena for allowing us to use the Yale PDS facility and Gary Da Costa for technical assistance during the measurements. We also wish to thank Takashi Nakajima and Arnold Klemola (University of California, Santa Cruz) for their work with the Lick Sky Survey plates, including AME measurements and reductions of proper motion. The referee provided comments that significantly improved the paper. This research was supported by grants from the National Science Foundation, the Anglo-Australian Telescope Board, and the Connecticut State University system.

REFERENCES

Cannon, R. D. 1970, MNRAS, 150, 293
Castellani, V., Chieffi, A., & Straniero, O. 1992, ApJS, 78, 517
Cousins, A. W. J. 1974, Monthly Notes Astron. Soc. South Africa, 33, 149
Fernie, J. D. 1963, AJ, 68, 780
Friel, E. D., & Janes, K. A. 1993, A&A, 267, 75
Graham, J. A. 1982, PASP, 94, 244
Jahn, K., Kaluzny, J., & Ruciński, S. M. 1995, A&A, 295, 101
King, I. 1964, R. Obs. Bull., 82, 106
Landolt, A. U. 1983, AJ, 88, 439
Lee, J.-F., & van Altena, W. F. 1983, AJ, 88, 1683
Nakajima, T. 1986, Master's thesis, San Diego State Univ.
Phelps, R. L., Janes, K. A., & Montgomery, K. A. 1994, AJ, 107, 1079
Trumpler, R. J. 1930, Lick Obs. Bull., 14, 154
Tsarevskii, G. S., & Abakumov, I. E. 1971, Astron. Tsirk., 631, 6
Twarog, B. A., Anthony-Twarog, B. J., & Hawarden, T. G. 1995, PASP, 107, 1215